

A novel hybrid approach to Baltic Dry Index forecasting based on a combined dynamic fluctuation network and artificial intelligence method



X. Zhang^{a,b,*}, M.Y. Chen^a, M.G. Wang^{c,d}, Y.E. Ge^a, H.E. Stanley^b

^aCollege of Transport and Communications, Shanghai Maritime University, Shanghai 201306, China

^bCenter for Polymer Studies and Department of Physics, Boston University, Boston, MA 02215, USA

^cSchool of Mathematical Science, Nanjing Normal University, Nanjing 210042, Jiangsu, China

^dDepartment of Mathematics, Nanjing Normal University Taizhou College, Taizhou 225300, Jiangsu, China

ARTICLE INFO

Keywords:

Artificial intelligence algorithm
Complex network
Dynamic fluctuation network
Baltic Dry Index prediction

ABSTRACT

Enhancing the accuracy of freight rate forecasting is crucial when agents in the shipping industry make their business decisions and strive to avoid or reduce possible risks. Although there has been a lot of freight rate trend analysis in the literature, the time-varying and volatile nature of the shipping market makes the accurate prediction of it extremely difficult, if not impossible. In this research, we first propose the use of a dynamic fluctuation network (DFN) to transform a time series data set into an evolving directed network, which removes the noise in the data and allows us to extract time-varying features in it. We then develop a hybrid approach that combines the DFN and artificial intelligence (AI) techniques to forecast the Baltic Dry Index (BDI), which is new to the literature. The utilization of DFN with AI enables the non-linear, cyclical and dynamic features of the BDI to be extracted effectively and the prediction accuracy is not impacted by the length and time-scale of sample selection either in long-term or short-term forecasting. These advantages of DFN offset the well-known limitations of traditional AI-based algorithms and econometric models in BDI forecasting. The empirical results from applying the resultant model to multi-time-scale datasets in a random sampling case show that the model is more accurate than the model based on the AI technique only. We test the accuracy of the DFN-AI model in three challenging cases which respectively contain a sudden rise, a decline, or frequent fluctuations of the BDI. The DFN-AI model has fewer errors and a higher trend matching rate than the corresponding AI-based model. Our hybrid approach also shows its superiority in working with data containing an extreme market downturn, which shed light on the predictability of BDI. This study has important implications for overall business, commercial, and hedging strategies in the shipping industry.

© 2019 Elsevier Inc. All rights reserved.

1. Introduction

International maritime transportation takes up between 80% and 90% of the volume of global commodity trade and contributes significantly to the welfare and development of many nations. Freight rates alone add approximately \$380 billion

* Corresponding author at: College of Transport and Communications, Shanghai Maritime University, Shanghai 201306, China.
E-mail address: zhangxin@shmtu.edu.cn (X. Zhang).

a year to the global economy. Because shipping freight rates are a considerable proportion of the price of finished goods, there is a strong relationship between shipping freight rates and wholesale prices that must be understood and predicted. [1,2].

The Baltic Dry Index (BDI) published by the Baltic Exchange is a “barometer” of shipping freights and is widely used as a major indicator in the shipping industry, world international trade, and global economy [3–7]. The BDI tracks the cost of such world-wide shipping commodities as coal, iron ore, steel, cement, and grain. Changes in the BDI are linked to changes in the prices of commodities, and thus the BDI is sensitive to the demand for raw materials and global trade as the behavior of commodity prices vary over the business cycle. The BDI can also reflect speculative movements, since there are futures contracts on BDI, and the underlying freight market can also reveal the speculative actions of market participants.

Thus forecasting BDI trends allows operators and investors to manage market trends and avoid risk in the shipping industry, and is also useful to industries and manufacturers in the world economic system [3,8]. Because such factors as market supply and demand [9], bunker price [10], and speculative trading [11] create high noise levels, the BDI exhibits such complex volatility characteristics as nonlinearity, cyclicity, and uncertainty [12–15]. Although predicting BDI trends is difficult, prediction accuracy is essential in large-scale organizations and firms because managerial decisions are based on perceived future prospects.

The variety of econometric time series forecasting models proposed in the literature exhibit such drawbacks in the BDI datasets as non-stationarity and non-linearity. In addition to the classic econometric approaches, artificial intelligence (AI) methods have been used in recent years to explore the inner complexity of BDI. Although AI methods can model such complex characteristics as nonlinearity and volatility so that are more accurate than econometric models, they also have disadvantages, e.g., they suffer from the local minimum point and over-fitting, and also are sensitive to parameter selection.

Because single predictive approach—including both econometric models and AI methods—are limited, many studies now use hybrid methods to forecast the BDI. Empirical analysis results consistently demonstrate that hybrid forecast methods are more accurate than single methods because hybrid methods combine single models and allow the merits of each to offset the defects of the others.

In recent years complex network theory has been widely used to analyze nonlinear time series. Complex network theory uses algorithms to transform a nonlinear time series into corresponding complex networks and uses a complex network typology to reveal regular fluctuation patterns. The application of complex network theory has been widely effective in determining the essential characteristics of a time series. Recently a large number of researchers have successfully applied complex network theory to the study of such time series as stock prices, crude oil prices, and trade volumes, which have produced valuable results [16–18].

The rapid development of complex network time series analysis thus provides a new perspective on how to eliminate noise in the original data, but there are fewer studies that apply complex network-based time series analysis to forecast BDI trends. We here combine complex network analysis and AI predictive methods to formulate a novel hybrid model for BDI forecasting. Empirical results demonstrate that the proposed dynamic fluctuation network (DFN) AI models (i.e., DFN-BP, DFN-RBF, and DFN-ELM) perform significantly better than their corresponding single AI models. Our proposed DFN-AI methods are also robust and can be flexibly applied to a broader prediction of freight rates, such as the freight rate of a specific route or of a certain vessel type.

The paper is organized as follows. The next section reviews previous research on the methodologies of BDI and other shipping freight rates forecasting. Section 3 introduces the dynamic fluctuation network and presents the forecasting procedure of DFN-AI model. Section 4 describes the original BDI data we use in our experimental prediction comparisons. Section 5 applies the proposed method to random sampling and challenging situation cases to demonstrate the improvement in accuracy of the DFN-AI models over the benchmark methods of the corresponding single AI models. The last section lists our conclusions and proposes possible directions for future research.

2. Literature review

Because of their uncertainty and volatility, freight rates and ways of qualitatively analyzing them have long been topics of interest in the shipping industry. There is a large and ever-growing body of literature proposing models that forecast shipping freight rates, many of which use the Baltic Dry Index [19,20]. The methodologies that use the Baltic Dry Index, among others, fall into three rough categories.

2.1 Univariate and multivariate econometric methods

The first includes univariate and multivariate econometric methods, such as the auto-regressive integrated moving average (ARIMA), vector auto-regression (VAR), generalized autoregressive conditional heteroskedasticity (GARCH), and vector error correction (VECM) models used to analyze and forecast shipping freight rates. Veenstra and Franses [21] use a cointegrated process of the time series and a unit root test to develop a VAR model for forecasting the BDI. Cullinane et al. [22] pioneered the use of the ARIMA model to test the effect of the new composition rule of BFI. Kavussanos and Alizadeh [23] use a seasonal single-variable autoregressive integral moving average model and a VAR model to study the seasonal characteristics of the dry bulk shipping market. Batchelor et al. [24] compare ARIMA, VAR, and VECM results when predicting spot and forward freight rates. Luo et al. [25] develop dynamic-economic models to predict the fluctuations in the

container freight rate based on the supply and demand factors in the container transportation service. Chen et al. [26] use ARIMA and VAR to predict the freight rates of several dry bulk routes and find that VAR performs better on the out-of-sample forecast than ARIMA. To improve the forecasting accuracy of the BDI, Tsioumas et al. [27] propose a multivariate VAR model with exogenous variables (VARX) that incorporates Chinese steel production, dry bulk fleet development, a new composite indicator, and the dry bulk economic climate index (DBECI), and they find that the VARX model outperforms the ARIMA approach. Chen et al. [28] focus on the correlation between pre-announcement of price increase and liner shipping spot rates by using an ordered logit model to analyze the impact of the external events in spot rate trend. Adland et al. [29] establish a cointegrated time series models in continuous and discrete time to analyze the dynamics of regional ocean freight rates.

2.2 Nonlinear and artificial intelligence (AI) methods

Stopford [30] reminds us that maritime forecasting has a poor reputation because it is difficult for traditional econometric and statistical methods to capture the nonlinear characteristics hidden in freight rates [31]. Thus in recent years a number of nonlinear and artificial intelligence (AI) methods, including artificial neural networks (ANN), support vector machines (SVM), and non-linear regression have been used. Li et al. [32] investigate the use of neural networks for the short and long-term prediction of monthly tanker freight rates and find that neural networks significantly outperform time series models, especially in longer-term forecasting. Yang et al. [33] use a support vector machine (SVM) to forecast the extreme fluctuations of CCBFI, CCFI, and BFI. Goulielmos and Psifia [34] develop a nonlinear method for testing the nonlinear dynamic and chaotic deterministic modeling theory. Thalassinos et al. [19] use chaos methodology to predict a BDI time series with invariant parameters of the reconstructed strange attractor that governs the evolution of the system. Guan et al. [35] propose an SVM-based forecasting model combining direct and iterative prediction and use a support vector machine (SVM), hybrid multistep prediction, and weekly BSI data to test the model's performance. Şahin et al. [36] compare the BDI forecasting accuracy of three different ANN models and find that their performances are similar, but that the most consistent is ANN using BDI input data from the two most-recent weekly observations.

These studies indicate that AI-based methods produce significantly better results than traditional econometric and statistical models. Although ANNs can better handle non-linear relationships that involve arbitrary complexity, strong robustness, and fault tolerance, the model structure of the AI algorithm is difficult to determine. It is also prone to excessive or insufficient training, and this induces shortages, such as trapping in the local minimum caused by a sensitivity to initial values.

2.3 Hybrid models

Hybrid models that combine interdisciplinary methods allow strengths to overcome limitations. The usual way of establishing a hybrid model is to integrate a noise reduction technique with an AI-based algorithm. Leonov and Nikolov [37] propose a model based on wavelets and neural networks to predict dry bulk freight rates. Bulut et al. [38] develop a vector autoregressive fuzzy integrated logical forecasting model for time charter rates. Duru et al. [39] propose a fuzzy-Delphi adjustment method to improve the accuracy of statistical forecasts of the dry bulk shipping index. Han et al. [40] use wavelet transform to denoise the BDI data series and combine wavelet transform and a support vector machine to forecast BDI. Zeng et al. [41] develop a method based on empirical mode decomposition (EMD) and artificial neural networks (ANN). Uyar et al. [42] develop a genetic-algorithm-based trained recurrent neural network to improve the accuracy of long-term freight rate index forecasting. Eslami et al. [43] develop a hybrid model based on an artificial neural network (ANN) and an adaptive genetic algorithm (AGA) for short-term prediction of tanker freight rates. They find that hybrid model is not only significantly superior to the regression approach and the moving average approach, but also slightly superior to existing ANN studies.

Empirical results show that the hybrid model has superiorities than single AI model in time series forecasting. Therefore, in future hybrid forecasting models will become the hot interests focus on the shipping freight market analysis. However, at the same time, the calculation process required in hybrid methods is complicated. The critical question is how to effectively reduce the high level of noise corrupting the freight rate data in the shipping market and thus largely weakening the prediction capability of AI-models.

3. Methodology

In this section, we first describe the DFN technique and then form a hybrid DFN-AI approach to forecast the BDI series. At last, three prediction accuracy measurements are proposed.

3.1. Dynamic fluctuation network (DFN)

Complex network theory has recently been used to analyze time series because it can characterize hidden time series features that are difficult for conservative econometric and statistical methods to capture. The approach encodes the dynamics of the time series into the topology of the corresponding network. Zhang and Small [44] first introduced this method by transforming a pseudo-periodic time series into a complex network. Bridging time series analysis and complex networks has yielded high-quality results in both theoretical and practical studies [45]. There are now a variety of algorithms for mapping

time series into complex networks, including the visibility graph (VG) [46,47], a pseudo-periodic time series transformation algorithm [48], a phase space reconstruction method [49], and a coarse-graining phase space method [50].

The dynamic fluctuation network (DFN) is a complex network-based time series transformation technique that can reveal the hidden characteristics and dynamics of time series. It thus can be used as a highly effective forecasting tool. A DFN maps the evolution of fluctuation modes in the original time series to a corresponding network and uses its topology to extract fluctuation features [16]. The DFN approach to reconstructing the original BDI includes the following steps:

(1) Calculate the fluctuation state series

From the original BDI time series $X = X(t)$ with $t = 0, 1, 2, \dots, N$ we obtain the return series $R = R(t)$ with $t = 1, 2, \dots, N$,

$$R(t) = \frac{X(t) - X(t-1)}{X(t-1)}, \quad (1)$$

where $X(0) = X(1)$ and thus $R(1) = 0$.

We next define $s(t)$ to be the fluctuation state of BDI at time t , according to return series $R(t)$ using indicator function $I(R)$,

$$s(t) = \begin{cases} s_1 & R(t) > r \\ s_2 & -r \leq R(t) \leq r, r = \frac{1}{N} \sum |R(t)| \\ s_3 & R(t) < -r \end{cases}. \quad (2)$$

The continuous return series $R(t)$ is thus transformed into discrete fluctuation state sequence $s(t)$ and $s(t) \in \{s_1, s_2, \dots, s_k\}$ with $k = 3$ symbol in our case. Here $s_1 = 1$, $s_2 = 0$, and $s_3 = -1$.

(2) Obtain the fluctuation mode

We use the sliding window method with a window length $L = 5$ and sliding step $l = 1$ and divide the fluctuation state sequence $s(t)$ into several overlapping sequences with a fixed length L . Each sequence is a fluctuation mode denoted S^m , $m = 1, 2, \dots, \hat{M}$. There are thus a total of $\hat{M} = [N - L + l]$ fluctuation modes, and the original state sequence can be rewritten to fluctuation mode matrix S ,

$$S = \begin{bmatrix} s(1) & s(2) & \cdots & s(\hat{M}) \\ \vdots & \vdots & \cdots & \vdots \\ s(L) & s(L+1) & \cdots & s(L+\hat{M}+1) \end{bmatrix} = [S^1, S^2, \dots, S^{\hat{M}}]. \quad (3)$$

Using the fluctuation state sequence shown in Fig. 1 as an example, the fluctuation state sequence is given as $s(t) = \{s_1, s_2, s_1, s_3, s_1, s_2, s_1, s_3, s_1\}$. After sliding the window with $L = 5$ and $l = 1$ the $s(t)$ is transferred to the fluctuation mode matrix S as follows,

$$S = \begin{bmatrix} s_1 & s_2 & s_1 & s_3 & s_1 \\ s_2 & s_1 & s_3 & s_1 & s_2 \\ s_1 & s_3 & s_1 & s_2 & s_1 \\ s_3 & s_1 & s_2 & s_1 & s_3 \\ s_1 & s_2 & s_1 & s_3 & s_1 \end{bmatrix} = [S^1, S^2, S^3, S^4, S^5]. \quad (4)$$

(3) Construct dynamic fluctuation network

To map the fluctuation mode matrix S to a dynamic fluctuation network, we denote the different fluctuation modes to be DFN nodes notated V_i , where $i = 1, 2, \dots, n$, and $n \leq \hat{M}$. Transformations among different fluctuation modes are edges between nodes. For example, when fluctuation mode i transforms to j there is a directed link from node V_i to node V_j . Thus while the fluctuating modes are evolving into each other in time, the directed fluctuation network $DFN(r, k, L, l)$ is being constructed. Fig. 1 shows a fluctuation mode matrix presented as a directed network with four nodes and four edges $N = \{V_1 \rightarrow V_2 \rightarrow V_3 \rightarrow V_4 \rightarrow V_1\}$.

(4) Extract the fluctuation features

Because the DFN is a directed network, all nodes except the first and last one all nodes have an in-neighbor and out-neighbor set.

In order to make a prediction, we aim the last fluctuation mode S^n in the data, which is the last column in fluctuation mode matrix S . We define the target node V_i^T to be the node that is mapped by the last fluctuation mode S^n . Fig. 1 shows that the last fluctuation mode S^5 is mapped to node V_1 . Thus the target node is V_1 and the set of its out-neighbors E_{V^T} is identified and is V_2 in Fig. 1. For arbitrary node V_i belong to the E_{V^T} , we can obtain one or more fluctuation modes mapped

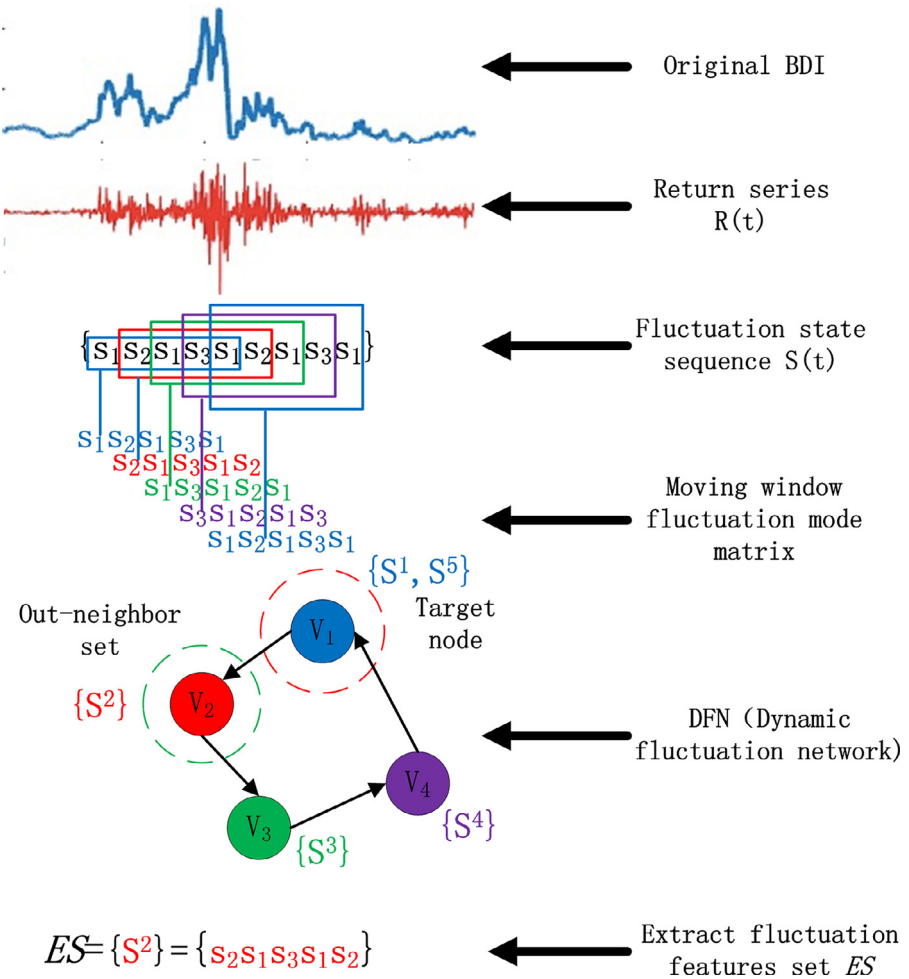


Fig. 1. The paradigm for the process of transforming original BDI data to dynamic fluctuation network (DFN) and to extract fluctuation features according to the topology of DFN.

to it. We thus can extract the fluctuation feature set ES containing all possible fluctuation modes that can evolve from the last fluctuation mode S^n at next time stamp,

$$ES = \begin{bmatrix} ES(1) & ES(2) & \dots & ES(D) \\ \vdots & \vdots & \ddots & \vdots \\ ES(L) & ES(L+1) & \dots & ES(L+D+1) \end{bmatrix}. \quad (5)$$

Fig. 1 shows that the out-neighbor set contains only node V_2 , and that fluctuation mode S^2 is mapped to V_2 . This thus generates the fluctuation features set $ES = \{S^2\} = \{s_2, s_1, s_3, s_1, s_2\}$.

3.2. DFN-AI approach for BDI forecasting

After using the dynamic fluctuation network to extract the fluctuation features we can formulate a novel hybrid DFN-AI forecasting approach for the BDI index. There are three steps in the proposed DFN-AI forecasting approach, (i) constructing the training dataset of the AI learning algorithm, (ii) normalizing and denormalizing data, and (iii) forecasting using AI algorithms.

STEP 1: Construct the training dataset of the AI learning algorithm

After determining the training and testing stages, we map the original BDI data of a given training stage on a directed DFN using the method described in Section 3.1. We then use the topological structure of the DFN to extract the fluctuation feature set ES of the BDI. We can either use this ES to directly identify the corresponding original BDI data ED to be the

input training dataset for the AI-learning algorithm. Or we can combine a subset SD of BDI data with ED identified by fluctuation feature set ES . Here the input data should be $[ED; SD]$. The way to extract SD could be varied according to different prediction requirements. Here we use a subset of original BDI data before the beginning of the testing stage with a length twice that of testing dataset SD and combine it with ED to construct the training dataset for the AI algorithm.

STEP 2: Data normalization and denormalization

AI-learning algorithm requires the preparation in data processing to minimize the difference between the threshold and actual data. Training data are usually normalized before being input,

$$x'_t = \frac{x_t - x_{\min}}{x_{\max} - x_{\min}}, \quad (6)$$

where x'_t is the data after normalization at time t , and x_{\min} and x_{\max} are the minimum and maximum of input x_t . After processing we need to anti-normalize the output,

$$\hat{y}_t = y'_t(y_{\max} + y_{\min}) + y_{\min} \quad (7)$$

where \hat{y}_t is the predictive data after anti-normalization at time t , and y_{\min} and y_{\max} are the minimum and maximum of output y'_t .

STEP 3: Forecasting using AI algorithms

After normalizing the training data, we use an AI learning algorithm to model the input training data and simulate the prediction results. A series of recently-developed AI learning algorithms for time series forecasting are clearly superior to traditional forecasting models [16,51]. Here we focus on three prevailing models, (i) the back propagation neural network (BP), (ii) the radial basis function neural network (RBF), (iii) and the extreme learning machine (ELM). For detailed descriptions of these three AI-based models see Appendix A.

We set BP, RBF, and ELM to be standard two-layer artificial neural network models with a hidden layer and an output layer. Note that a small number of hidden neurons causes inaccuracies in the correlation between inputs and outputs and that a large number produces local optimums. Hastie et al. [52] find that, because the typical number of nodes is in the 5 to 100 range, using cross-validation is unnecessary. We thus set the parameters as follows.

For BP we set the number of nodes in the hidden layer to the default value of the 'newff' command in MATLAB, and we set the other training parameters $\text{net.trainParam.epochs} = 1000$, $\text{net.trainParam.goal} = 1e-6$, and $\text{net.trainParam.lr} = 0.01$. For RBF we set the number of nodes in the hidden layer to 90 and the radial basis function to the Gaussian function. For ELM we set the number of nodes in the hidden layer to be 8.

3.3. Accuracy measurements

To measure the forecasting accuracy of these proposed methods, we apply the widely-used error measurements of mean absolute percentage error (MAPE) and root mean square error (RMSE) methods [53,54], defined

$$MAPE = \frac{1}{N} \sum_{t=1}^N \left| \frac{X(t) - \hat{X}(t)}{X(t)} \right| \quad (8)$$

and

$$RMSE = \sqrt{\frac{\sum_{t=1}^N (\hat{X}(t) - X(t))^2}{N}}, \quad (9)$$

where $\hat{X}(t)$ and $X(t)$ are the predicted and real values at time t , respectively, and N is the size of the dataset being tested. The MAPE measures the mean absolute relative error of the prediction models, and the RMSE measures their standard deviation. The smaller the MAPE and RMSE values the greater the level of model accuracy.

For a given prediction, actual outcomes above and below the prediction are treated asymmetrically in MAPE and RMSE [55]. Thus we must know the directional tendency of the data fluctuations—whether they are upward, stable, or downward—and we measure them using the direction matching rate $Dsta$, defined

$$Dsta = \frac{1}{N} \sum_{t=1}^N a(t), \quad (10)$$

and

$$a(t) = \begin{cases} 1, & (X(t+1) - X(t)) * (\hat{X}(t+1) - X(t)) \geq 0 \\ 0, & \text{otherwise} \end{cases}. \quad (11)$$

The closer the $Dsta$ value is to 1, the higher the accuracy of the directional prediction of the models, and the closer the $Dsta$ value is to 0, the lower the accuracy of their directional predictions.

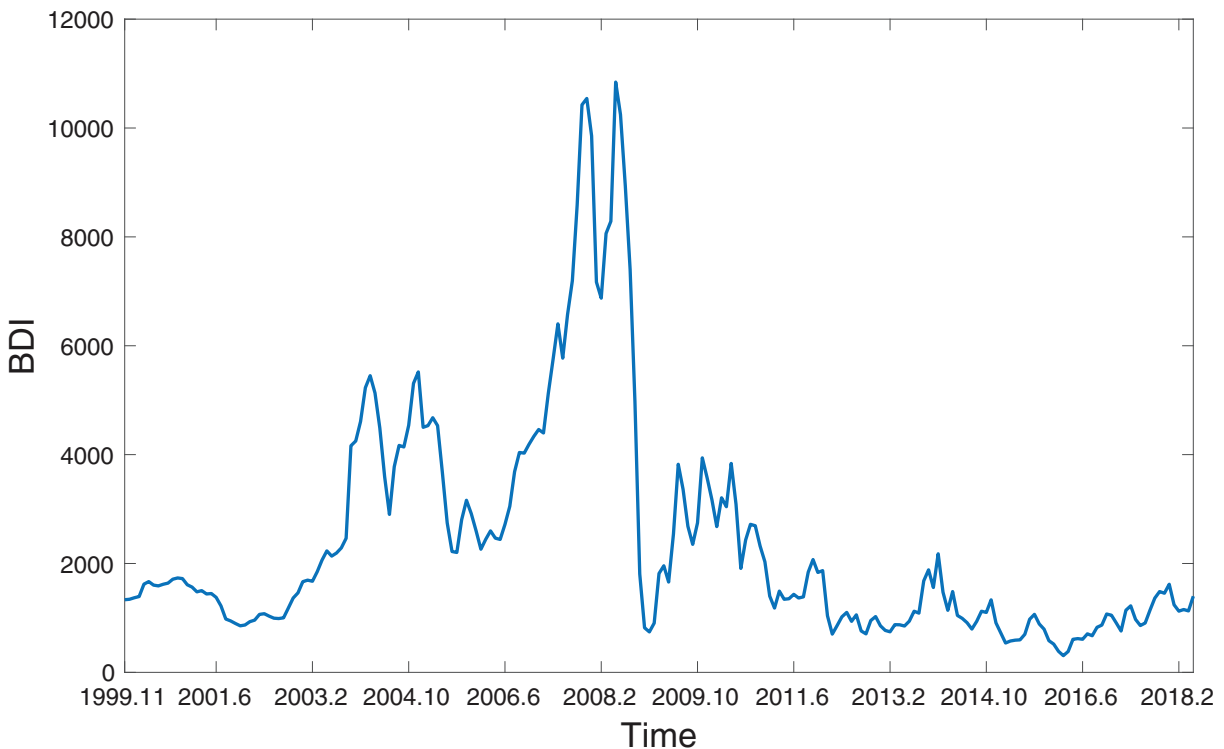


Fig. 2. Trend of daily BDI dataset used to make prediction.

4. Data

To meet the requirements of participants of the dry bulk shipping market, the Baltic Freight Index (BFI) began to be published in 1985 by the London Baltic Exchange. On 1 November 1999 the BDI replaced the BFI, and it is now widely used by industry practitioners and regarded an important economic indicator. The BDI is a daily index that takes into consideration 26 shipping routes measured on a time-charter and voyage basis, which is a composite of three sub-indices that measure different sized dry bulk carriers and merchant ships: Capesize, Panamax, and Supramax. We here use the daily, weekly, and monthly BDI data from 1 November 1999 to 30 February 2018 as our experimental datasets when comparing forecasting accuracy. All datasets are from the world's leading shipping database Clarkson Sin (<https://sin.clarksons.net/>).

Fig. 2 shows that the BDI fluctuations are large in amplitude, high in frequency, and irregular. From November 1999 to early in 2003 the BDI value fluctuated gently, and market volatility began to increase in 2003. On 20 May 2008 the BDI had reached 11,793 but in the following six months it dropped sharply to approximately 700 points.

Note that for BDI stable periods are surrounded by periods of extreme volatility. Periods with sustained large rate increases are followed by stable periods lasting a few months. A cluster of downward moves brings the process back to an average upward drift. Shipping decisions made by ship owners and charter firms are strongly affected by expected trend of the BDI, which are associated with the time of entering charter contracts, their duration, switching between spot and time charter operations, improving hedging performance using derivative contracts, and also when to invest in newly-built or second-hand vessels.

5. Empirical results

5.1. Forecasting results in random sampling cases

To analyze the robustness of our hybrid DFN-AI model, we use daily, weekly and monthly datasets. For the sake of analysis and comparison, in each dataset we randomly select 100 sample data from five different time periods for training and testing. Utilizing previous research, we set the size ratio between training and testing sets to be 8: 2. In our predicting we apply DFN-BP, DFN-RBF, and DFN-ELM and their corresponding single models. We then measure the prediction accuracy of each forecasting model by calculating the MAPE, RMSE, and Dsta. Finally we evaluate the improvement in accuracy to be the difference between the accuracy of the DFN-AI model and the corresponding single AI model divided by the value of accuracy measurement of a single AI model.

Table 1

Performance improvement percentage of DFN-AI models compared to corresponding AI models for daily BDI prediction.

Stage	Method	Performance improvement percentage		
		MAPE	RMSE	Dsta
Training: 1999/11/12-2000/4/10 Testing: 2000/4/11-2000/5/11	DFN-BP	27.6%	22.6%	20.0%
	DFN-RBF	52.3%	46.3%	5.9%
	DFN-ELM	82.2%	77.8%	70.0%
	DFN-BP	10.3%	4.7%	30.0%
Training: 2000/8/18-2001/1/11 Testing: 2001/1/12-2001/2/8	DFN-RBF	40.5%	38.0%	33.3%
	DFN-ELM	78.6%	100.0%	14.3%
	DFN-BP	36.6%	24.2%	6.7%
	DFN-RBF	22.0%	20.6%	5.6%
Training: 2005/6/7-2005/10/26 Testing: 2005/10/27-2005/11/23	DFN-ELM	46.8%	35.6%	0.0%
	DFN-BP	25.0%	20.2%	28.6%
	DFN-RBF	6.8%	8.5%	5.3%
	DFN-ELM	23.8%	25.5%	12.5%
Training: 2008/8/15-2009/1/13 Testing: 2009/1/14-2009/2/10	DFN-BP	50.4%	42.4%	26.7%
	DFN-RBF	41.9%	32.6%	18.8%
	DFN-ELM	85.6%	82.1%	111.1%

Table 2

Performance improvement percentage of DFN-AI models compared to corresponding AI models for weekly BDI prediction.

Stage	Method	Performance improvement percentage		
		MAPE	RMSE	Dsta
Training: 1999/12/3-2001/11/16 Testing: 2001/11/17-2002/4/5	DFN-BP	38.2%	33.2%	9.1%
	DFN-RBF	72.7%	68.9%	87.5%
	DFN-ELM	90.3%	100.0%	57.1%
	DFN-BP	12.5%	8.1%	7.1%
Training: 2002/4/5-2004/3/5 Testing: 2004/3/6-2004/7/23	DFN-RBF	61.1%	59.0%	20.0%
	DFN-ELM	53.3%	50.2%	133.3%
	DFN-BP	44.5%	34.2%	100.0%
	DFN-RBF	20.0%	11.6%	0.0%
Training: 2003/9/12-2005/8/19 Testing: 2005/8/20-2006/1/13	DFN-ELM	68.3%	61.8%	33.3%
	DFN-BP	40.6%	33.3%	116.7%
	DFN-RBF	4.3%	4.2%	18.2%
	DFN-ELM	34.8%	29.1%	50.0%
Training: 2009/2/13-2011/1/28 Testing: 2011/1/29-2011/6/17	DFN-BP	69.1%	60.1%	36.4%
	DFN-RBF	26.1%	15.4%	30.0%
	DFN-ELM	80.5%	73.1%	27.3%

5.1.1. Daily BDI forecasting

We use as sample data the daily Baltic dry bulk index from 1 November 1999 to 18 May 2018. To verify the extent to which the DFN-AI models can be generalized, we randomly select 100 sample data, use the previous 80 sample data (80%) as training samples, and use the remaining 20 sample data (20%) as testing samples. The original training samples are selected in five different periods.

Table 1 compares the percentage of performance improvement of three DFN-AI models with their corresponding single AI algorithms as the baseline models. When the improvement percentage is positive, the DFN-AI model outperforms the corresponding single AI model, and the higher the value the more significant the improvement.

Note that in all five random sampling stages, the predictive performance both in errors and direction matching are improved by introducing DFN. The predictions of the DFN-AI models are more accurate than those of traditional single AI models. The average improvement percentage in the MAPE of DFN-BP, DFN-RBF, and DFN-ELM are 29.98%, 32.64%, and 64.3%, respectively, and of Dsta are 20.04%, 13.78%, and 41.58%, respectively. Thus DFN-ELM exhibits the most significant improvement levels. We compare the predictive performances in detail in **Table B.1** of Appendix B.

5.1.2. Weekly BDI forecasting

Because previous studies indicate that data frequency strongly affects BDI forecasting accuracy, we use weekly data from 5 November 1999 to 18 May 2018 to measure the improvement in forecasting accuracy of the DFN-AI models. **Table 2** compares the performance improvement percentage of DFN-AI models with their baseline single AI model. Similar to daily BDI predictions, performance improvement percentages are positive in all sampling stages and in all three model types compared. Thus using DFN to extract fluctuation features of the original time series in an AI-based prediction enhances accuracy. The average improvement percentage in MAPE of DFN-BP, DFN-RBF, and DFN-ELM are 40.98%, 28.84%, and 65.44%, respectively, and of Dsta are 53.86%, 31.14%, and 60.14%, respectively. Compared to daily data, DFN exhibits the same improvement

Table 3

Performance improvement percentage of DFN-AI models compared to corresponding AI models for monthly BDI prediction.

Stage	Method	Performance improvement percentage		
		MAPE	RMSE	Dsta
Training: 2003/12-2010/8 Testing: 2010/9-2012/4	DFN-BP	37.8%	26.4%	30.0%
	DFN-RBF	27.6%	3.4%	30.0%
	DFN-ELM	27.3%	11.5%	0.0%
	DFN-BP	42.8%	23.5%	18.2%
Training: 2005/3-2011/11 Testing: 2011/12-2013/7	DFN-RBF	16.1%	11.5%	9.1%
	DFN-ELM	28.8%	9.3%	30.0%
	DFN-BP	34.2%	12.4%	62.5%
Training: 2006/1-2012/9 Testing: 2012/10-2014/5	DFN-RBF	24.3%	5.9%	40.0%
	DFN-ELM	28.5%	4.0%	33.3%
	DFN-BP	55.5%	41.7%	20.0%
Training: 2008/2-2014/10 Testing: 2014/11-2016/6	DFN-RBF	34.2%	20.7%	50.0%
	DFN-ELM	44.2%	30.1%	36.4%
	DFN-BP	9.6%	3.6%	7.1%
Training: 2008/12-2015/8 Testing: 2015/9-2017/4	DFN-RBF	16.7%	19.1%	9.1%
	DFN-ELM	24.6%	3.4%	11.1%

level for the weekly BDI prediction. Moreover, the improvement in directional matching rate for all three DFN-AI models is more significant in the weekly BDI predictions than in the daily data forecasting. For a predictive performance comparison of weekly BDI in detail, see [Table B.2](#) of Appendix B.

5.1.3. Monthly BDI forecasting

Because using low-frequency time scale data to make long-term BDI predictions is challenging, we examine how DFN can increase the accuracy of monthly data forecasting. We use the same predictive approach as for daily and weekly data. We randomly choose 100 observations to be our sample and divide it into training data and testing data according to the ratio 8: 2. [Table 3](#) lists the percentages of predictive performance improvement of DFN-AI models to single AI models in five stages. Note that the DFN approach enhances the accuracy significantly, and that the average improvements of MAPE for BP, RBF, and ELM are 35.98%, 23.78%, 30.68%, respectively. In addition, the MAPE values of the monthly data of all single AI forecasting models are over 0.2 (see [Table B.3](#) in Appendix B), indicating that they fail to predict monthly BDI. After applying DFN, the MAPE of all three AI forecasting models are equal to or less than 0.2, indicating that they are good prediction models (See [Table B.3](#) of Appendix B).

5.2. Forecasting results in challenging situations

We examine the improvement in predictive performance of the DFN-AI in a random sampling case, and we determine whether the DFN approach yields the same increase in accuracy under challenging and abnormal situations. We thus here select three typical challenging conditions and compare the predictive performance of our DFN-AI models with that of non-hybrid AI models for both daily and weekly BDI datasets. [Fig. 3](#) show the training and testing periods of three challenging situations.

Situation I: forecasting a sudden price surge

From 1999 to the second quarter of 2003, the BDI fluctuated between 1000 and 2000 points, but it then increased by 52% from 2900 to 4500 points in October 2003. That began a boom period in the world dry bulk shipping market that lasted until the 2008 worldwide financial crisis. We choose training data from 15 August 2002 to 15 September 2003 with 270 daily data observations and 54 weekly data observations. We select testing data from 16 September 2003 to 27 October 2003 with 30 daily data observations and 6 for weekly data observations.

Situation II: predict the sudden decline of BDI.

Following the rapid growth period from 2004 to 2007, the shipping market plummeted in the 2008 worldwide financial crisis. Over a six-month period, the BDI dropped from approximately 10,000 points to a historic low of roughly 1000 points. Since that time the world shipping market has remained weak, despite a global recovery in trade and the economy. For the training dataset in this situation, we use the BDI from 13 September 2005 to 22 May 2008 in which the daily predictions include 420 observations and the weekly 84 observations. For the testing dataset, we use the BDI from 23 May 2008 to 24 November 2008 in which the daily predictions include 130 observations and the weekly 26 observations.

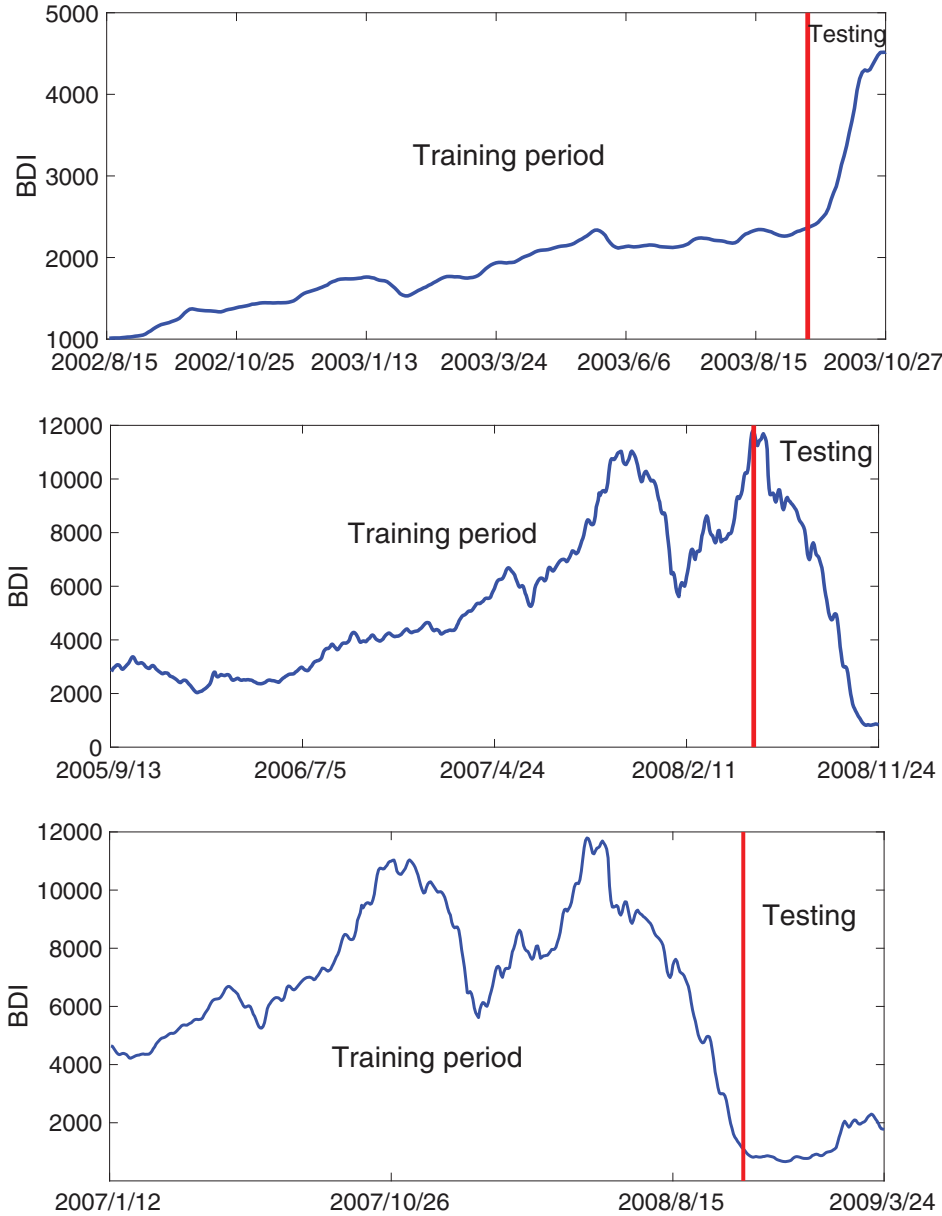


Fig. 3. Training and testing dataset of BDI for challenging situation I (top), situation II (central) and situation III (bottom).

Situation III: predict the turning points of frequent fluctuations

In addition to sharp increases and decreases, the BDI also exhibits extreme high-frequency fluctuations. For example, following 2008 plunge, BDI fluctuated between 1000 and 2000 points during the first and second quarters of 2009. For the training data, we thus use the BDI from 12 January 2007 to 12 January 2009 in which the daily predictions include 500 observations and the weekly 100 observations. For the testing dataset, we use the BDI from 24 March 2007 to 26 March 2008 in which the daily predictions include 200 observations and the weekly 40 observations.

We first examine the daily BDI dataset. Fig. 4 compares the actual BDI values with the predicted values generated by three DFN-AI models and their corresponding single AI models in the three testing situations. The inset in each figure shows the zoomed in detail of a particular period marked by the red circle.

We find that both the DFN-AI models and the single AI models predict the trend in three situations, but the predicted values generated by the DFN-AI models deviate less from the actual BDI. For example, in situation I beginning in October 2003 the ELM and RBF predictions deviate, but the DFN-RBF and DFN-ELM predictions are still very close to the actual BDI

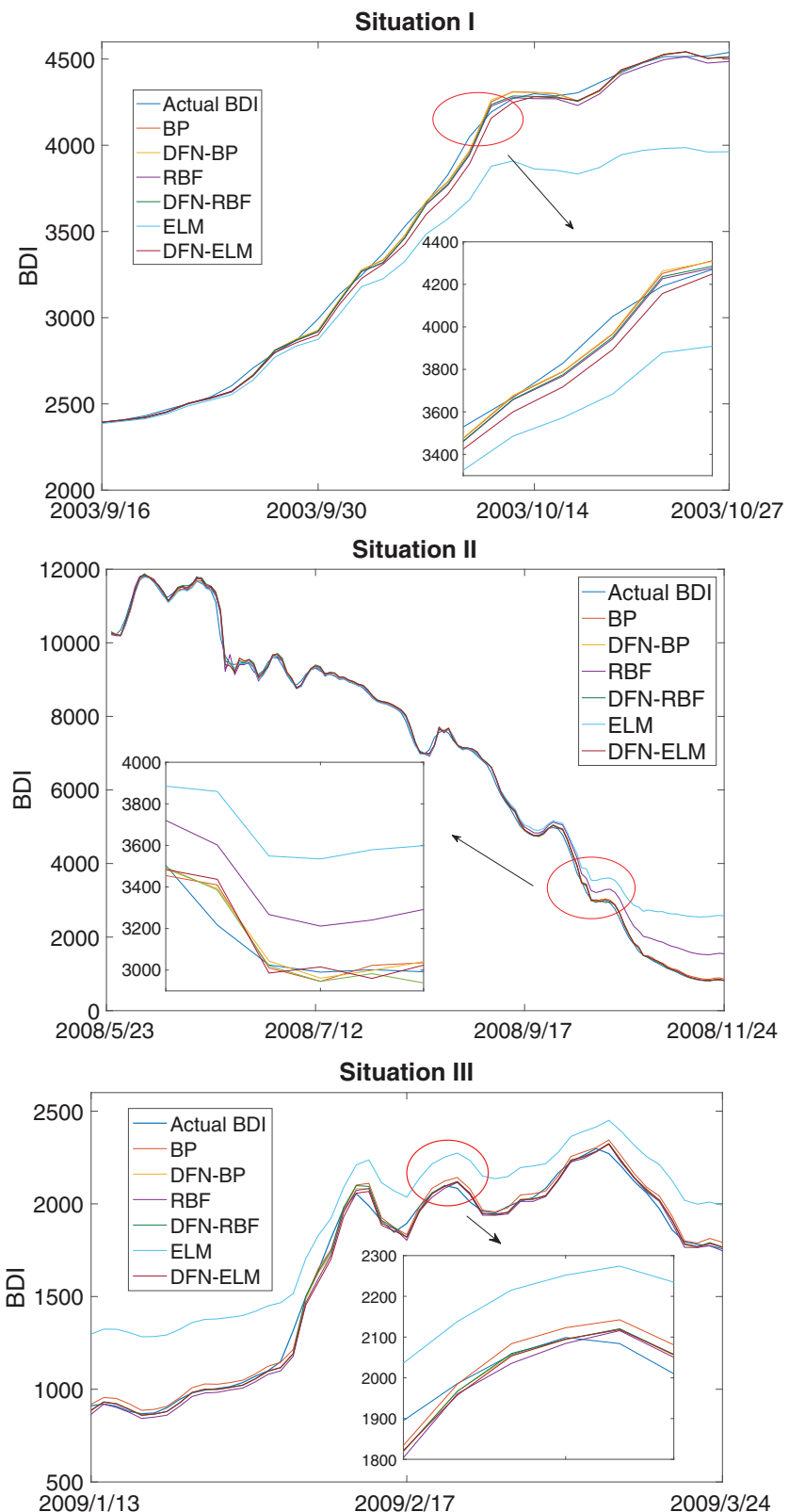


Fig. 4. Actual BDI and forecasting results through three DFN-AI models and their corresponding AI models for daily data in situation I (Top), situation II (Central) and situation III (Bottom).

Table 4

Performance improvement percentage of DFN-AI models compared to corresponding AI models for daily BDI prediction in three challenging situations

Stage	Method	Performance improvement percentage		
		MAPE	RMSE	Dsta
Training: 2002/8/15-2003/9/15	DFN-BP	0.3%	2.0%	0.0%
	DFN-RBF	8.6%	12.8%	2.3%
Testing: 2003/9/16-2003/10/27	DFN-ELM	84.1%	89.5%	13%
	DFN-BP	63.2%	4.8%	22.9%
Training: 2005/9/13-2008/5/22	DFN-RBF	95.9%	76.3%	41.6%
	DFN-ELM	98.2%	90.8%	42.3%
Testing: 2008/5/23-2008/11/24	DFN-BP	37.7%	7.9%	18.1%
	DFN-RBF	22.9%	2.0%	10.6%
Training: 2007/1/12-2009/1/12	DFN-ELM	96.9%	90.8%	93.7%
Testing: 2009/1/13-2009/3/24				

Table 5

Performance improvement percentage of DFN-AI models compared to corresponding AI models for weekly BDI prediction in three challenging situations.

Stage	Method	Performance improvement percentage		
		MAPE	RMSE	Dsta
Training: 2002/8/15-2003/9/15	DFN-BP	38.71%	35.37%	33.33%
	DFN-RBF	54.28%	61.29%	100.00%
Testing: 2003/9/16-2003/10/27	DFN-ELM	72.45%	75.98%	252.00%
	DFN-BP	11.81%	8.14%	24.62%
Training: 2005/9/13-2008/5/22	DFN-RBF	17.19%	4.34%	6.90%
	DFN-ELM	61.20%	25.90%	7.41%
Testing: 2008/5/23-2008/11/24	DFN-BP	64.89%	28.75%	-2.82%
	DFN-RBF	48.21%	5.46%	0.00%
Training: 2007/1/12-2009/1/12	DFN-ELM	85.73%	66.47%	7.81%
Testing: 2009/1/13-2009/3/24				

values. We see similar behavior in situation II at the end of September 2008. **Table 4** compares the improvements in the accuracy of the DFN-AI models with those of their corresponding single AI models.

Table 4 shows a positive performance improvement percentage in all three challenging cases, which indicates that that DFN increases forecasting accuracy under extreme circumstances. DFN-AI models outperform single AI models the most when predicting sudden drops. Using DFN narrows the predictive errors of all three AI models by more than 50% and increases the direction matching rates by more than 20%. For a detailed accuracy performance listing of the DFN-AI and single AI models, see **Table B.4** of Appendix B.

We next examine the weekly BDI dataset and determine how much the DFN-AI models improve prediction accuracy. **Fig. 5** compares the actual BDI value with the predicted value generated by DFN-AI models and their corresponding single AI models. The single AI model predictions of weekly data exhibit large errors, and the trends they predict are wrong. In contrast, the DFN-AI forecasting model reproduces BDI trends and displays relatively few errors. For example, in situation III the predicted values of single AI models deviate widely from BDI values, but the predicted values of DFN-AI models are very close to the BDI values.

Table 5 shows that in most circumstances DFN-AI decreases errors, increases the direction matching rate, and thus produces more accurate prediction results than single AI model. The only exception is in situation III when by using DFN the Dsta decreases by 2.82%. But compared to the improvement level in MAPE and RMSE, the decrease is very slight.

6. Concluding remarks

This paper aims to enhance the forecasting accuracy of the BDI by formulating a DFN-AI forecasting approach, which is a novel hybrid that can remove the noise in the data by combining dynamic fluctuation network (DFN) technique with artificial intelligence (AI) algorithms. Random sampling cases and challenging situations are designed to evaluate the forecasting accuracy improvement of DFN-AI compared to its corresponding single AI model. In this setting, the hybrid AI algorithms and single AI models are both used to generate forecasts for the same sample size and over the same horizon. In addition, we conduct daily, weekly, and monthly BDI predictions to test the performance robustness of DFN-AI models for different time scales.

The main intellectual merits of this work include the novel approach based on BDN and AI techniques and as an effective method for capturing non-linear and non-stationary characteristics of shipping freight market. The empirical results demonstrate that DFN-AI models yield lower forecasting errors and higher directional matching rates compared to corresponding single AI models. In addition, we validate the robustness of the accuracy improvement provided by DFN-AI models in both random sampling and challenging situations and for different BDI time-scale datasets. We find that the DFN-AI technique is

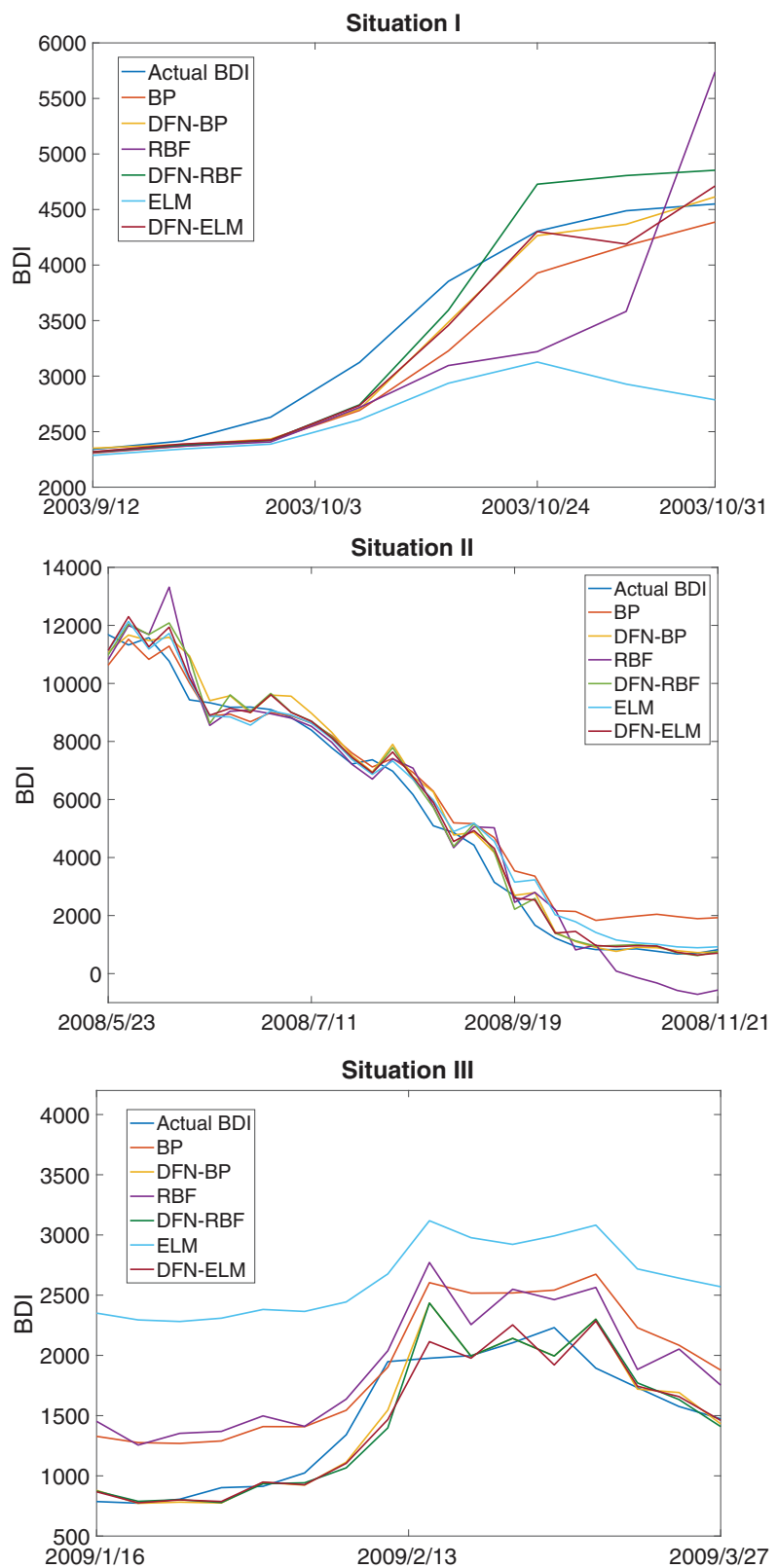


Fig. 5. Actual BDI and forecasting results through three DFN-AI models and their corresponding AI models for weekly data in situation I (Top), situation II (Central) and situation III (Bottom).

a promising tool for the accurate prediction of the BDI index, that its forecasting power is unaffected by training and testing sample selection, and that it is robust with respect to data frequency and extreme market switch.

This newly-proposed approach can serve as a useful tool for chartering and ship-building decisions under uncertainty. Shipping market practitioners can benefit from the satisfactory performance of this proposed forecasting approach and integrate it into their managerial toolkit. Our proposed approach and findings also extend freight rates forecasting research and suggest possible future roads of research in related fields.

Acknowledgments

This work was supported by the [National Science Foundation of China](#) (Grant no.: [71601112](#)), and the Shanghai Pujiang Program (Grant no.: [15PJ061](#)). The Boston University Center for Polymer Studies is supported by [NSF](#) Grants [PHY-1505000](#), [CMMI-1125290](#), and [CHE-1213217](#), by [DTRA](#) Grant [DTRAHDTRA1-14-1-0017](#), and by [DOE](#) Contract [DE-AC07-05Id14517](#). M.G. Wang thanks the support from the [National Science Foundation of China](#) (Grant no.: [71503132](#) and [71811520710](#)).

Appendix A

A series of artificial intelligence algorithms for time series forecasting were recently developed, and they have proven to be superior to traditional forecasting models. Here we focus on three prevailing models, (i) the back propagation neural network (BP), (ii) the radial basis function neural network (RBF), (iii) and the extreme learning machine (ELM).

1. Back propagation neural network (BP)

The back propagation neural network (BP) model is one of the most widely used artificial neural network algorithms for classification and prediction. This technique is an advanced multiple regression analysis that deals with responses that are more complex and non-linear than those of standard regression analysis. The basic formula of the BP algorithm is

$$W(n) = W(n - 1) - \Delta W(n), \quad (\text{A.1})$$

where

$$\Delta W(n) = \eta \frac{\partial E}{\partial W}(n - 1) + \gamma \Delta W(n - 1), \quad (\text{A.2})$$

where W is the weight, η is the learning rate, E is the gradient of error function, and $\gamma \Delta W(n - 1)$ is the incremental weight. Because the BPNN uses the gradient method the learning convergent velocity is slow, and a convergence to the local minimum always occurs. In addition, the selection of the learning and inertial factors affects the convergence of the BP, which is determined by the level of experience. Thus the usefulness of the BP is limited.

2. Radial basis function neural network (RBF)

The radial basis function network (RBF) is an artificial neural network using radial basis functions for activation. RBF networks typically have three layers: an input layer, a hidden layer with a non-linear RBF activation function, and a linear output layer. The input can be modeled as a vector of real numbers $x \in \mathbb{R}^r$, and the prototype of the input vectors $B_i \in \mathbb{R}^r$. The output of each RBF unit is

$$R_i(X) = R_i(\|X - B_i\|), i = 1, 2, \dots, u, \quad (\text{A.3})$$

where $\|\cdot\|$ is the Euclidean norm on the input space. Because it can be factored, the Gaussian function is the preferred radial basis function. Thus

$$R_i(X) = \exp\left[-\frac{\|X - B_i\|^2}{\sigma_i^2}\right], \quad (\text{A.4})$$

where σ_i is the width of RBF unit i . The output $Y_j(X)$ of unit j of an RBF is

$$Y_j(X) = \sum_{i=1}^u R_i(X) * W(j, i), \quad (\text{A.5})$$

where $R_0 = 1$, $W(j, i)$ is the weight or strength of receptive field i to output j , and $W(j, 0)$ is the bias of output j . Geometrically, an RBF partitions the input space into several hypersphere subspaces. The parameters of the RBF networks are the center, the influence field of the radial function, and the output weight between the neurons of the intermediate layer and those of the output layer. The training process produces these parameters.

3. The extreme learning machine

The extreme learning machine (ELM) was originally applied to single hidden-layer feed-forward neural networks and then extended to generalized feed-forward networks. For a set of training samples $(X_j, C_j)_{j=1}^N$ with N samples and C classes, the single hidden layer feed-forward neural network with h hidden nodes and activation function $f(x)$ is

$$\sum_{i=1}^h \beta_i f_i(X_j) = \sum_{i=1}^h \beta_i f(W_i * X_j + b_i) = Y_j, \quad j = 1, 2, \dots, N, \quad (\text{A.6})$$

where $X_j = [x_{j1}, x_{j2}, \dots, x_{jm}]^T$, $C_j = [c_{j1}, c_{j2}, \dots, c_{jm}]^T$, $W_j = [w_{j1}, w_{j2}, \dots, w_{jm}]^T$, and b_i are the input, its corresponding output, the connecting weights of hidden neuron i to input neurons, and the bias of hidden node i , respectively, and $\beta_j = [\beta_{j1}, \beta_{j2}, \dots, \beta_{jm}]^T$ are the connecting weights of hidden neuron i to output neurons, and Y_j the actual network output with respect to input X_j . Because the hidden parameters W_i , b_i can be randomly generated during the training period without tuning, ELM solves a compact model that minimizes the error between C_j and Y_j , i.e., $\min \|H\beta - C\|_F$.

Here H is the hidden layer output matrix and β the output weight matrix. The merit of ELM is that only the output weights are needed when randomly selecting the hidden node parameters (input weights and bias).

Appendix B

1. Predictive performance comparision in random sampling case

In the random sampling case, we randomly select 100 sample data and use the previous 80 sample data (80%) as training samples and the remaining 20 sample data (20%) as testing samples. The original training samples are selected in five different periods. To predict we apply DFN-BP, DFN-RBF, and DFN-ELM and their corresponding single models for daily, weekly and monthly BDI datasets. Then for each forecasting model we calculate MAPE, RMSE, and Dsta to measure the predictive accuracy. Tables B.1 to B.3 compare the predictive performance of the proposed DFN-AI models and their corresponding single AI models for daily, weekly, and monthly BDI data.

Table B.1
Predictive performance of daily BDI in random sampling case.

Stage	Method	MAPE	RMSE	Dsta
Training: 1999/11/12-2000/4/10 Testing: 2000/4/11-2000/5/11	BP	0.00192	3.90198	0.75
	DFN-BP	0.00139	3.02902	0.90
	RBF	0.00281	5.38122	0.85
	DFN-RBF	0.00134	2.89125	0.90
	ELM	0.00767	13.75021	0.50
	DFN-ELM	0.00137	3.05009	0.78
	BP	0.00199	4.08437	0.50
	DFN-BP	0.00179	3.89923	0.65
	RBF	0.00276	5.88549	0.45
	DFN-RBF	0.00164	3.65093	0.60
Training: 2000/8/18-2001/1/11 Testing: 2001/1/12-2001/2/8	ELM	0.00802	13.46265	0.70
	DFN-ELM	0.00171	11.61286	0.60
	BP	0.01025	35.54588	0.75
	DFN-BP	0.00650	26.93127	0.80
	RBF	0.00857	33.46903	0.90
	DFN-RBF	0.00668	26.58556	0.85
	ELM	0.01196	40.94235	0.80
	DFN-ELM	0.00636	26.36093	0.80
	BP	0.01934	19.19007	0.70
	DFN-BP	0.01451	15.30635	0.90
Training: 2005/6/7-2005/10/26 Testing: 2005/10/27-2005/11/23	RBF	0.01394	15.08657	0.95
	DFN-RBF	0.01489	16.36838	0.90
	ELM	0.01946	21.22951	0.80
	DFN-ELM	0.01483	15.81096	0.90
	BP	0.01081	10.34134	0.75
	DFN-BP	0.00536	5.95278	0.95
	RBF	0.00899	9.00304	0.80
	DFN-RBF	0.00522	6.07135	0.95
	ELM	0.03614	32.97336	0.45
	DFN-ELM	0.00520	5.89394	0.95

Table B.2
Predictive performance of weekly BDI in random sampling case.

Stage	Method	MAPE	RMSE	Dsta
Training: 1999/12/3-2001/11/16 Testing: 2001/11/17-2002/4/5	BP	0.04236	46.57877	0.55
	DFN-BP	0.02616	31.11013	0.60
	RBF	0.10225	110.05158	0.40
	DFN-RBF	0.02787	34.22540	0.75
	ELM	0.32349	327.43545	0.35
	DFN-ELM	0.03151	0.03151	0.55
	BP	0.04269	282.54217	0.70
	DFN-BP	0.03736	260.14876	0.75
	RBF	0.17308	1114.48357	0.50
	DFN-RBF	0.06726	454.52055	0.60
Training: 2002/4/5-2004/3/5 Testing: 2004/3/6-2004/7/23	ELM	0.09507	594.28247	0.30
	DFN-ELM	0.04444	295.80142	0.70
	BP	0.09122	280.93011	0.35
	DFN-BP	0.05065	185.02082	0.70
	RBF	0.05922	206.93379	0.70
	DFN-RBF	0.04736	182.84187	0.70
	ELM	0.15724	476.81562	0.60
	DFN-ELM	0.04978	181.88049	0.80
	BP	0.08755	198.13938	0.30
	DFN-BP	0.05198	132.37173	0.65
Training: 2003/9/12-2005/8/19 Testing: 2005/8/20-2006/1/13	RBF	0.06262	168.21386	0.55
	DFN-RBF	0.05995	161.42761	0.65
	ELM	0.07555	182.05714	0.40
	DFN-ELM	0.04929	129.28527	0.60
	BP	0.09577	64.04353	0.55
	DFN-BP	0.02959	25.55870	0.75
	RBF	0.04377	33.46092	0.50
	DFN-RBF	0.03234	28.30832	0.65
	ELM	0.14746	95.93572	0.55
	DFN-ELM	0.02872	25.78082	0.70

Table B.3
Predictive performance of monthly BDI in random sampling case.

Stage	Method	MAPE	RMSE	Dsta
Training: 2003/12-2010/8 Testing: 2010/9-2012/4	BP	0.25313	428.58006	0.50
	DFN-BP	0.15737	315.25122	0.65
	RBF	0.26440	436.87125	0.50
	DFN-RBF	0.19149	452.47002	0.65
	ELM	0.24232	398.77113	0.60
	DFN-ELM	0.17625	352.73889	0.60
	BP	0.27635	323.12399	0.55
	DFN-BP	0.15803	247.31021	0.65
	RBF	0.22948	280.68354	0.55
	DFN-RBF	0.19242	248.52451	0.60
Training: 2005/3-2011/11 Testing: 2011/12-2013/7	ELM	0.22907	283.26009	0.50
	DFN-ELM	0.16308	257.05023	0.65
	BP	0.23708	397.38009	0.40
	DFN-BP	0.15601	348.20023	0.65
	RBF	0.26273	428.13229	0.50
	DFN-RBF	0.19884	403.03931	0.70
	ELM	0.22360	362.29357	0.45
	DFN-ELM	0.15977	347.64344	0.60
	BP	0.42771	282.77128	0.50
	DFN-BP	0.19035	164.92001	0.60
Training: 2006/1-2012/9 Testing: 2012/10-2014/5	RBF	0.31660	221.60356	0.50
	DFN-RBF	0.20829	175.66878	0.75
	ELM	0.33990	232.80922	0.55
	DFN-ELM	0.18965	162.78034	0.75
	BP	0.19010	147.76996	0.70
	DFN-BP	0.17179	153.30001	0.75
	RBF	0.24456	206.79023	0.55
	DFN-RBF	0.20368	167.32334	0.60
	ELM	0.23445	167.09054	0.45
	DFN-ELM	0.17677	161.49934	0.50

Table B.4
Predictive performance of daily BDI in challenging situations.

Stage	Method	MAPE	RMSE	Dsta
Training: 2002/8/15-2003/9/15 Testing: 2003/9/16-2003/10/27	BP	0.00341	19.18578	0.89
	DFN-BP	0.00340	18.80553	0.89
	RBF	0.00381	23.12751	0.87
	DFN-RBF	0.00348	20.17087	0.89
	ELM	0.02685	267.91125	0.77
	DFN-ELM	0.00426	28.03865	0.87
	BP	0.03423	103.15406	0.72
	DFN-BP	0.01259	98.25412	0.89
	RBF	0.26696	409.52739	0.63
	DFN-RBF	0.01201	96.91043	0.89
Training: 2007/1/12-2008/5/22 Testing: 2008/5/23-2008/11/24	ELM	0.64715	977.38720	0.62
	DFN-ELM	0.01181	90.28075	0.88
	BP	0.02347	61.81627	0.75
	DFN-BP	0.01461	56.92212	0.88
	RBF	0.01946	59.04360	0.80
	DFN-RBF	0.01501	57.87757	0.89
	ELM	0.50432	639.40416	0.58
	DFN-ELM	0.01545	59.09879	0.88

Table B.5
Predictive performance of weekly BDI in challenging situations.

Stage	Method	MAPE	RMSE	Dsta
Training: 2002/8/15-2003/9/15 Testing: 2003/9/16-2003/10/27	BP	0.07601	334.28185	0.75
	DFN-BP	0.04659	216.06056	1.00
	RBF	0.14468	724.74624	0.50
	DFN-RBF	0.06615	280.55880	1.00
	ELM	0.19474	1006.86782	0.25
	DFN-ELM	0.05366	241.80484	0.88
	BP	0.09962	499.61321	0.81
	DFN-BP	0.08785	543.87804	0.65
	RBF	0.21657	722.42213	0.58
	DFN-RBF	0.17934	691.08259	0.62
Training: 2005/9/13-2008/5/22 Testing: 2008/5/23-2008/11/24	ELM	0.32401	794.64852	0.54
	DFN-ELM	0.12570	588.84270	0.58
	BP	0.29589	479.91840	0.71
	DFN-BP	0.10390	341.96185	0.69
	RBF	0.32643	503.77855	0.67
	DFN-RBF	0.16906	476.26261	0.67
	ELM	0.84728	1084.39283	0.64
	DFN-ELM	0.12090	363.58595	0.69

2. Predictive performance comparision in challenging situation

We choose three typical challenging situations, a sudden rise, a fall, and frequent fluctuations of BDI and compare the predictive performance of our DFN-AI models with that of non-hybrid AI models for both daily and weekly BDI forecasts. Tables B.4 and B.5 list the predictive performances of DFN-AI and single AI models for daily and weekly BDI forecasting, respectively.

References

- [1] F. Papailias, D.D. Thomakos, J. Liu, The Baltic Dry Index: cyclicalities, forecasting and hedging strategies, *Empir. Econ.* 52 (1) (2017) 255–282.
- [2] G. Giannarakis, C. Lemonakis, A. Sormas, C. Georganakis, et al., The effect of Baltic Dry Index, gold, oil and usa trade balance on dow jones sustainability index world, *Int. J. Econ. Financ. Issues* 7 (5) (2017) 155–160.
- [3] N. Apergis, J.E. Payne, New evidence on the information and predictive content of the Baltic Dry Index, *Int. J. Financ. Stud.* 1 (3) (2013) 62–80.
- [4] F. Lin, N.C. Sim, Trade, income and the Baltic Dry Index, *Eur. Econ. Rev.* 59 (2013) 1–18.
- [5] A.H. Alizadeh, G. Muradoglu, Stock market efficiency and international shipping-market information, *J. Int. Financ. Mark. Inst. Money* 33 (2014) 445–461.
- [6] N.C. Papapostolou, P.K. Pouliasis, N.K. Nomikos, I. Kyriakou, Shipping investor sentiment and international stock return predictability, *Transp. Res. Part E Logist. Transp. Res.* 96 (2016) 81–94.
- [7] M.E. Bildirici, F. Kayıkçı, I.Ş. Onat, Baltic Dry Index as a major economic policy indicator: the relationship with economic growth, *Proc. Soc. Behav. Sci.* 210 (2015) 416–424.
- [8] Y. Wang, Q. Meng, Y. Du, Liner container seasonal shipping revenue management, *Transp. Res. Part B Methodol.* 82 (2015) 141–161.
- [9] J. Randers, U. Göluke, Forecasting turning points in shipping freight rates: lessons from 30 years of practical effort, *Syst. Dyn. Rev. J. Syst. Dyn. Soc.* 23 (2–3) (2007) 253–284.
- [10] Q. Ruan, Y. Wang, X. Lu, J. Qin, Cross-correlations between Baltic Dry Index and crude oil prices, *Phys. A Stat. Mech. Appl.* 453 (2016) 278–289.

- [11] S. Albertijn, W. Bessler, W. Drobetz, Financing shipping companies and shipping operations: a risk-management perspective, *J. Appl. Corp. Finance* 23 (4) (2011) 70–82.
- [12] X. Ding, S. Dai, F. Chen, Y. Miao, K. Tian, Y. Zeng, H. Xu, C. Qin, Long memory and scaling behavior study of bulk freight rate volatility with structural breaks, *Transp. Lett.* 10 (2017) 1–11.
- [13] J. Liu, F. Chen, Asymmetric volatility varies in different dry bulk freight rate markets under structure breaks, *Phys. A Stat. Mech. Appl.* 505 (2018) 316–327.
- [14] F. Chen, K. Tian, Y. Miao, X. Ding, et al., Multifractal characteristics in maritime economics volatility, *Int. J. Transp. Econ.* 44 (3) (2017a) 365–380.
- [15] Y. Kou, M. Luo, Y. Zhao, Examining the theoretical-empirical inconsistency on stationarity of shipping freight rate, *Marit. Policy Manag.* 45 (2) (2018) 145–158.
- [16] M. Wang, L. Zhao, R. Du, C. Wang, L. Chen, L. Tian, H.E. Stanley, A novel hybrid method of forecasting crude oil prices using complex network science and artificial intelligence algorithms, *Appl. Energy* 220 (2018b) 480–495.
- [17] R. Zhang, B. Ashuri, Y. Deng, A novel method for forecasting time series based on fuzzy logic and visibility graph, *Adv. Data Anal. Classif.* 11 (4) (2017) 759–783.
- [18] L. Lacasa, V. Nicosia, V. Latora, Network structure of multivariate time series, *Sci. Rep.* 5 (2015) 15508.
- [19] E.I. Thalassinos, M.P. Hanias, P.G. Curtis, J.E. Thalassinos, Forecasting financial indices: The baltic dry indices, *Marine Navigation and Safety of Sea Transportation: STCW, Maritime Education and Training (MET), Human Resources and Crew Manning, Maritime Policy, Logistics and Economic Matters*, 2013, p. 283.
- [20] G. Alexandridis, M.G. Kavussanos, C.Y. Kim, D.A. Tsouknidis, I.D. Visvikis, A survey of shipping finance research: Setting the future research agenda, *Transp. Res. Part E Logist. Transp. Rev.* 115 (2018) 164–212.
- [21] A.W. Veenstra, P.H. Franses, A co-integration approach to forecasting freight rates in the dry bulk shipping sector, *Transp. Res. Part A Policy Pract.* 31 (6) (1997) 447–458.
- [22] K. Cullinane, K. Mason, M. Cape, A comparison of models for forecasting the baltic freight index: Box-Jenkins revisited, *Int. J. Marit. Econ.* 1 (2) (1999) 15–39.
- [23] M.G. Kavussanos, A.H. Alizadeh-M, Seasonality patterns in dry bulk shipping spot and time charter freight rates, *Transp. Res. Part E Logist. Transp. Rev.* 37 (6) (2001) 443–467.
- [24] R. Batchelor, A. Alizadeh, I. Visvikis, Forecasting spot and forward prices in the international freight market, *Int. J. Forecast.* 23 (1) (2007) 101–114.
- [25] M. Luo, L. Fan, L. Liu, A dynamic-economic model for container freight market, in: Proceedings of the Department of Logistics and Maritime Studies at the Hong Kong Polytechnic University, Hong Kong, Presented at the International Association of Maritime Economists (IAME) Conference on June, 2009, pp. 24–26.
- [26] S. Chen, H. Meersman, E. Van de Voorde, Forecasting spot rates at main routes in the dry bulk market, *Marit. Econ. Logist.* 14 (4) (2012) 498–537.
- [27] V. Tsiontas, S. Papadimitriou, Y. Smirlis, S.Z. Zahran, A novel approach to forecasting the bulk freight market, *Asian J. Shipp. Logist.* 33 (1) (2017) 33–41.
- [28] G. Chen, N.G. Rytter, L. Jiang, P. Nielsen, L. Jensen, Pre-announcements of price increase intentions in liner shipping spot markets, *Transp. Res. Part A Policy Pract.* 95 (2017b) 109–125.
- [29] R. Adland, F.E. Benth, S. Koekebakker, Multivariate modeling and analysis of regional ocean freight rates, *Transp. Res. Part E Logist. Transp. Rev.* 113 (2018) 194–221.
- [30] M. Stopford, *Maritime Economics*, Routledge, 2013.
- [31] S. Dai, Y. Zeng, F. Chen, The scaling behavior of bulk freight rate volatility, *Int. J. Transp. Econ.* 43 (1/2) (2016) 85–104.
- [32] J. Li, M.G. Parsons, Forecasting tanker freight rate using neural networks, *Marit. Policy Manag.* 24 (1) (1997) 9–30.
- [33] H. Yang, F. Dong, M. Ogandaga, Forewarning of freight rate in shipping market based on support vector machine, in: *Traffic and Transportation Studies*, 2008, pp. 295–303.
- [34] A.M. Goulielmos, M.-E. Psifia, Forecasting weekly freight rates for one-year time charter 65000 dwt bulk carrier, 1989–2008, using nonlinear methods, *Marit. Policy Manag.* 36 (5) (2009) 411–436.
- [35] F. Guan, Z. Peng, K. Wang, X. Song, J. Gao, Multi-step hybrid prediction model of baltic supermax index based on support vector machine, *Neural Netw. World* 26 (3) (2016) 219.
- [36] B. ŞAHİN, S. GÜRGEN, B. ÜNVER, İ. ALTIN, Forecasting the Baltic Dry Index by using an artificial neural network approach, *Turk. J. Electr. Eng. Comput. Sci.* 26 (3) (2018) 1673–1684.
- [37] Y. Leonov, V. Nikolov, A wavelet and neural network model for the prediction of dry bulk shipping indices, *Marit. Econ. Logist.* 14 (3) (2012) 319–333.
- [38] E. Bulut, O. Duru, S. Yoshida, A fuzzy integrated logical forecasting (filf) model of time charter rates in dry bulk shipping: a vector autoregressive design of fuzzy time series with fuzzy c-means clustering, *Marit. Econ. Logist.* 14 (3) (2012) 300–318.
- [39] O. Duru, E. Bulut, S. Yoshida, A fuzzy extended delphi method for adjustment of statistical time series prediction: an empirical study on dry bulk freight market case, *Expert Syst. Appl.* 39 (1) (2012) 840–848.
- [40] Q. Han, B. Yan, G. Ning, B. Yu, Forecasting dry bulk freight index with improved SVM, *Math. Probl. Eng.* 2014 (2014) 1–12.
- [41] Q. Zeng, C. Qu, A.K. Ng, X. Zhao, A new approach for Baltic Dry Index forecasting based on empirical mode decomposition and neural networks, *Marit. Econ. Logist.* 18 (2) (2016) 192–210.
- [42] K. Uyar, A. İlhan, et al., Long term dry cargo freight rates forecasting by using recurrent fuzzy neural networks, *Proc. Comput. Sci.* 102 (2016) 642–647.
- [43] P. Eslami, K. Jung, D. Lee, A. Tjolleng, Predicting tanker freight rates using parsimonious variables and a hybrid artificial neural network with an adaptive genetic algorithm, *Marit. Econ. Logist.* 19 (3) (2017) 538–550.
- [44] J. Zhang, M. Small, Complex network from pseudoperiodic time series: topology versus dynamics, *Phys. Rev. Lett.* 96 (23) (2006) 238701.
- [45] Z.-K. Gao, M. Small, J. Kurths, Complex network analysis of time series, *EPL (Europhys. Lett.)* 116 (5) (2017) 50001.
- [46] L. Lacasa, B. Luque, F. Ballesteros, J. Luque, J.C. Nuno, From time series to complex networks: The visibility graph, *Proc. Natl. Acad. Sci.* 105 (13) (2008) 4972–4975.
- [47] M. Wang, A.L. Vilela, R. Du, L. Zhao, G. Dong, L. Tian, H.E. Stanley, Exact results of the limited penetrable horizontal visibility graph associated to random time series and its application, *Sci. Rep.* 8 (1) (2018a) 5130.
- [48] X. Sun, M. Small, Y. Zhao, X. Xue, Characterizing system dynamics with a weighted and directed network constructed from time series data, *Chaos Interdiscip. J. Nonlinear Sci.* 24 (2) (2014) 024402.
- [49] Z. Gao, N. Jin, Complex network from time series based on phase space reconstruction, *Chaos Interdiscip. J. Nonlinear Sci.* 19 (3) (2009) 033137.
- [50] S.H. Strogatz, *Nonlinear Dynamics and Chaos: with Applications to Physics, Biology, Chemistry, and Engineering*, CRC Press, 2018.
- [51] Z. Ghahramani, *Probabilistic machine learning and artificial intelligence*, Nature 521 (7553) (2015) 452.
- [52] T. Hastie, R. Tibshirani, J. Friedman, *Unsupervised learning*, in: *The Elements of Statistical Learning*, Springer, 2009, pp. 485–585.
- [53] A. De Myttenaere, B. Golden, B. Le Grand, F. Rossi, Mean absolute percentage error for regression models, *Neurocomputing* 192 (2016) 38–48.
- [54] E.W. Steyerberg, A.J. Vickers, N.R. Cook, T. Gerds, M. Gonen, N. Obuchowski, M.J. Pencina, M.W. Kattan, Assessing the performance of prediction models: a framework for some traditional and novel measures, *Epidemiol. (Cambridge, Mass.)* 21 (1) (2010) 128.
- [55] J. McKenzie, Mean absolute percentage error and bias in economic forecasting, *Econ. Lett.* 113 (3) (2011) 259–262.